Annals of the University of Craiova, Mathematics and Computer Science Series
Volume 46(1), 2019, Pages 109–124
ISSN: 1223-6934

Numerical resolution of Richards equation by the RBF-MQ method

P. O. Fabrice Ouédraogo, W. Olivier Sawadogo, and Oussséni So

Abstract. In this paper, the flow equation in unsaturated porous media is numerically integrated using the RBF-MQ method which is a meshless method. The conservative form which is a pressure-content method was considered. The Richards equation being strongly non-linear, we used Newton-Raphson's iterative method for linearisation. A implicit Euler scheme was used for temporal discretization. Comparison with exacts solution and experimental cases existing in the literature have shown the effectiveness of the approach.

2010 Mathematics Subject Classification. 65M06,65M70,76S05.
Key words and phrases. Unsaturated porous media, Richards equation, RBF-MQ method, implicit Euler scheme, Newton-Raphson method.

1. Introduction

The water flow problem in unsaturated porous media has long been of great interest to the scientific community and remains a hot topic especially for the community of hydrogeologists ([2],[4],[3],[6]). This problem is often associated with the problem of polluant transport as well as the problem of evaluating the water balance of the soil. The equation governing the flow of water in an unsaturated porous medium was defined by Richards in 1931 [2]. It is the result of the combination of the Darcy's law [1] and the conservation equation of the mass. The Richard's equation exist mainly in three forms: the pressure head h formulation, the formulation in moisture content θ and the mixed formulation pressure-content $\theta - h$.

Few analytical solutions of Richard's equation exist. This is related on the one hand to the fact that each analytic solution is specific to an given initial condition and on the other hand to the mathematical complexity of the Richard's equation itself. On the other hand, numerically, several solutions have been proposed by several authors and following various methods: the finite difference method ([3],[8]), the finite volume method ([7], [34]), the finite element method, the mixed finite element method ([9], [10]) and the discontinuous finite element [6]. Theses methods are based on the mesh of the domain in which the problem must be discretized. The mesh must obey certain rules. For example, the elements should not be overwritten to prevent the associated Jacobian from degenerating. This makes their implementation difficult and expensive ins some cases. To overcome these shortcomings, meshless methods have been developed since the 1970s. The idea is to reconstruct a function defined on a continuous space from the set of discrete values taken by this function on a not connected point cloud of the physical domain.

This paper has been presented at the Conference MOCASIM, Marrakesh, 26-27 November 2018.

Radial basis function (RBF) methods are meshless methods that are widely used today in engineering and the approximation of partial differential equations (PDEs) approximation. Kansas ([16],[15]) was among the first to successfully use it to solve parabolic, elliptic and hyperbolic PDEs. Since then, several authors have used them to solve PDEs ([27],[28],[29]).

Stevens and Power [26] used a implicit RNF method to solve the pressure h formulation of Richards equation. More recently, F. Motaman and al. [23] used the RBF-DQ method to solve the moisture content θ formulation. These two formulations have limits. Indeed the resolution of the pressure formulation, in many cases leads to a significant error on the mass balance. The resolution of the formulation in water content, involves problems of discontinuity. In addition this latter form is only restricted to unsaturated media [3]. On the other hand, the numerical solutions, obtained with the mixed formulation are more precise. Moreover, it can be adapted to the saturation case ([3], [24], [25]).

In this work, we present the numerical resolution by the RBF-MQ method of the mixed formulation of Richards equation. The solutions obtained were compared with analytical solutions and experimental solutions.

The remaining work will be as follows: The second part is devoted to the presentation of the RBF-MQ method. The third part is devoted to solving the mixed formulation of the Richards equation by the RBF-MQ method. In a fourth part, we present the results obtained and finally we will make a conclusion which constitutes the fifth part of our work.

2. The RBF methods

The basic radial functions (RBF) appeared in the early 1970s in the approximation of scattered and multivariate data and interpolations of functions [12]. For the mathematical community, it is in 1982 that RBFs were introduced for the first time thanks to the works of Franke [14]. The use of RBFs in the resolution of PDEs began in 1990 with the works of Kansa ([16], [15]).

Since these works, several techniques of approximation of the PDEs based on the RBFs have been developed by researchers and more particularly during the last decade.

2.1. Definition. Let Φ be a function defined from $\mathbb{R}^d$ to $\mathbb{R}$, and let $c_j,\ j = 1, 2, \ldots, N$ be a set of point in $\mathbb{R}^d$. Φ is said to be a radial basis function if Φ is symmetric with respect to $c_j,\ j = 1, 2, \ldots, N$, for the Euclidean norm, i.e.

$$\forall (x, y) \in \mathbb{R}^d \times \mathbb{R}^d,\ \|x - c_j\| = \|y - c_j\| \Rightarrow \Phi(x) = \Phi(y).$$

The table 1 gives some examples of very common infinite derivable RBF functions. RBF Multiquadratique (MQ) was first used by Hardy [17] in 1971 who implemented the first RBF scheme in dimension 2 to approach geographic areas and the Thin-Plat Spline (TPS) some time after in 1977 by Duchon [18].

In this work, we opt for the spatial numerical approximation of functions, the RBF-MQ. This function provide spectral approximation [19] and can be performed easily.

The multiquadratic of Hardy (MQ)	$\phi(r,c)=\sqrt{r^2+c^2}$
The inverse multiquadratic (IMQ)	$\phi(r,c)=1/\sqrt{r^2+c^2}$
The inverse quadratic (IQ)	$\phi(r,c)=1/(r^2+c^2)$
The gaussian splines	$\phi(r,c)=e^{-(r^2/c^2)}$
The thin plate splines (TPS)	$\phi(r)=r^2\ln r$

TABLE 1. Example of infinitely differentiable RBFs

2.2. Principle. We consider a real valued function $u(x), x\in\mathbb{R}^d$ where d is the space dimension. The RBF collocation method consists of approximating u with a function $\hat{u}$ of the form

$$\hat{u}(x)=\sum_{j=1}^{N}\lambda_j\phi(\|x-x_j\|,c),\quad x\in\mathbb{R}^d \tag{1}$$

where the points $x_j,\ j=1,\dots,M$ are the *centers* of the RBF approximation, ϕ is a basic radial function and c the precision parameter. Expansion coefficients $\lambda_j,\ j=1,\dots,M$ are determined by setting:

$$\sum_{j=1}^{M}\lambda_j\phi(\|x_i-x_j\|,c)=u(x_i),\quad i=1,\dots,M.$$

Which is expressed in the following matrix form:

$$A\lambda=U \tag{2}$$

where

$$\lambda=(\lambda_1,\lambda_2,\dots,\lambda_M)^\top,\qquad U=(u(x_1),u(x_2),\dots,u(x_M))^\top$$

and

$$A=\begin{pmatrix}\phi(\|x_1-x_1\|,c) & \phi(\|x_1-x_2\|,c) & \dots & \dots & \phi(\|x_1-x_M\|,c)\\ \phi(\|x_2-x_1\|,c) & \phi(\|x_2-x_2\|,c) & \dots & \dots & \phi(\|x_2-x_M\|,c)\\ \vdots & \vdots & \ddots & & \vdots\\ \vdots & \vdots & & \ddots & \vdots\\ \phi(\|x_M-x_1\|,c) & \phi(\|x_M-x_2\|,c) & \dots & \dots & \phi(\|x_M-x_M\|,c)\end{pmatrix}$$

In [19], it is shown that if the RBF ϕ is the multiquadratic, then the interpolation matrix A is always nonsingular. Thus we have the expression of λ as following

$$\lambda=A^{-1}U. \tag{3}$$

The k order derivative of $\hat{u}$ at the center x_i is:

$$\frac{\partial^k\hat{u}(x_i)}{\partial x^k}=\sum_{j=1}^{M}\lambda_j\frac{\partial^k}{\partial x^k}\phi(\|x_i-x_j\|,c),\quad i=1,2,\dots,M. \tag{4}$$

In matrix form , the derivative (4) is written as :

$$U^{(k)}=A^{(k)}\lambda \tag{5}$$

with

$$U^{(k)}=\left(\frac{\partial^k\hat{u}(x_1)}{\partial x^k},\frac{\partial^k\hat{u}(x_2)}{\partial x^k},\dots,\frac{\partial^k\hat{u}(x_M)}{\partial x^k}\right)$$

and

$$A^{(k)} = \begin{pmatrix} \frac{\partial^k}{\partial x^k}\phi(\|x_1 - x_1\|, c) & \frac{\partial^k}{\partial x^k}\phi(\|x_1 - x_2\|, c) & \dots & \dots & \frac{\partial^k}{\partial x^k}\phi(\|x_1 - x_M\|, c) \\ \frac{\partial^k}{\partial x^k}\phi(\|x_2 - x_1\|, c) & \frac{\partial^k}{\partial x^k}\phi(\|x_2 - x_2\|, c) & \dots & \dots & \frac{\partial^k}{\partial x^k}\phi(\|x_2 - x_M\|, c) \\ \vdots & \vdots & \ddots & & \vdots \\ \vdots & \vdots & & \ddots & \vdots \\ \frac{\partial^k}{\partial x^k}\phi(\|x_M - x_1\|, c) & \frac{\partial^k}{\partial x^k}\phi(\|x_M - x_2\|, c) & \dots & \dots & \frac{\partial^k}{\partial x^k}\phi(\|x_M - x_M\|, c) \end{pmatrix} \tag{6}$$

If we replace λ by its expression in the equation (5), we get:

$$U^{(k)} = D^{(k)}U \tag{7}$$

where

$$D^{(k)} = A^{(k)}A^{-1}. \tag{8}$$

3. Resolution of the Richards equation in space dimension 1 by the RBF-MQ method

In this section, we present the numerical resolution of the mixed form of the Richards equation using Hardy's multi-quadratic basic radial function (RBF-MQ) for spatial discretization. The implicit Euler method was used for temporal discretization. Since the Richards equation is nonlinear, Newton's iterative method is used to solve the nonlinearity problem.

3.1. Problem to solve. Let $\Omega = [a, b], \subset \mathbb{R}$ be a spatial domain of study. Ω represents a column of water infiltration. $\partial\Omega = \{a, b\}$ is the edge of Ω and $\partial\Omega_D$, $\partial\Omega_N$ are the subsets of $\partial\Omega$ where Dirichlet and Neumann type boundary conditions are respectively applied. $[0, T]$ is the time interval for observing water flow..
The mixed form of Richards equation is given by:

$$\frac{\partial\theta(h)}{\partial t} + \frac{\partial}{\partial z}q(h) = f \quad \text{in} \quad \Omega \times [0, T] \tag{9}$$

$$q(h) = -K(h)\frac{\partial h}{\partial z} - K(h) \quad \text{in} \quad \Omega \times [0, T] \tag{10}$$

$$h = h_{init} \quad \text{in} \quad \Omega \tag{11}$$

$$h = g_D \quad \text{on} \quad \partial\Omega_D \times [0, T] \tag{12}$$

$$q(h) = g_N \quad \text{on} \quad \partial\Omega_N \times [0, T] \tag{13}$$

$h[L]$ is the unknown function and represent the pressure head. θ is the moisture content. $K(h)$ is the unsaturated hydraulic conductivity $q(h)$ is the flow velocity, g_D and g_N are respectively imposed pressure and flow on the boundaries $\partial\Omega_D$ and $\partial\Omega_N$. h_{init} is the initial pressure head. f is a source function.

3.2. Space approximation of the Richards equation by the RBF-MQ method. Let $\{z_i\}_{1\leqslant i\leqslant M}$ a set of points of Ω considered as centers. At each center z_i the approximation value $\hat{h}$ of the pressure head h by the RBF-MQ method is written as following:

$$\hat{h}(z_i, t) = \sum_{j=1}^{M} \lambda_j(t)\phi(\|z_i - z_j\|, c), \quad t \in]0, T] \tag{14}$$

where ϕ is the Multiquadratic function given in the table 1.
As in the expression (2), the expression (14) can be rewritten in matrix form

$$\mathbf{h} = A\ \lambda(t), \quad t \in]0, T] \tag{15}$$

where $\mathbf{h} = (h(z_1, t), h(z_2, t), \ldots, h(z_M, t))^\top$ and $\lambda(t) = (\lambda_1(t), \lambda_2(t), \ldots, \lambda_M(t))^\top$.

To obtain the first order derivative $\mathbf{h}^{(1)}$ of $\mathbf{h}$, we use the formula (7) in which the value of k is taken equal to one.

$$\mathbf{h}^{(1)} = D^{(1)}\mathbf{h}, \tag{16}$$

It is also possible to directly approximate the flow velocity $q(h)$ by RBF as following:

$$q \circ \hat{h}(z_i, t) = \sum_{j=1}^{M} \gamma_j(t)\phi(\|z_i - z_j\|, c), \quad t \in]0, T],\ z_i,\ i = 1, 2, \ldots, M$$

Where $\gamma_j(t),\ j = 1, 2, \ldots, M$ the expansion coefficients of $q(h)$.
This gives the matrix form

$$\mathbf{q}(\mathbf{h}) = A\ \Gamma(t), \quad t \in]0, T] \tag{17}$$

where $\Gamma(t) = (\gamma_1(t), \gamma_2(t), \ldots, \gamma_M(t))^\top$.
The derivative of $\mathbf{q}(\mathbf{h}, t)$ is also obtained by using the formula (7) in which the value of k taken to be equal to one:

$$\mathbf{q}^{(1)}(\mathbf{h}) = D^{(1)}\mathbf{q}(\mathbf{h}). \tag{18}$$

Now we will focus on the expression of $q(h)$ in the equation (10).
Based on the approximation $\hat{h}$ of h in the formula (14), we have the approximation of $q(h)$ at any center $z_i,\ i = 1, 2, \ldots, M$ as following:

$$q \circ \hat{h}(z_i, t) = -K \circ \hat{h}(z_i, t)\frac{\partial \hat{h}(z_i, t)}{\partial z} - K \circ \hat{h}(z_i, t), \quad t \in]0, T].$$

This can be rewritten in the matrix form

$$\mathbf{q}(\mathbf{h}, t) = -\mathbf{K}_D(\mathbf{h}, t)D^{(1)}\mathbf{h}(t) - \mathbf{K}(\mathbf{h}, t), \quad t \in]0, T] \tag{19}$$

where

$$\mathbf{K}(\mathbf{h}) = (K \circ \mathbf{h}_1, K \circ \mathbf{h}_2, , \ldots, K \circ \mathbf{h}_M,)^\top$$

et

$$\mathbf{K}_D(\mathbf{h}) = \begin{pmatrix} K \circ \mathbf{h}_1 & & & \\ & K \circ \mathbf{h}_2 & 0 & \\ & 0 & \ddots & \\ & & & K \circ \mathbf{h}_M \end{pmatrix}$$

with $\mathbf{h}_i = h(z_i, t),\ i = 1, \ldots, M,\ t \in]0, T]$ the ith value of the vector $\mathbf{h}$ (15).

Now that we have obtained the matrix expression of the approximation of the flow velocity $q(h)$ we replace it in the expression (18) to get the approximate matrix expression of the variation $\frac{\partial}{\partial z}q(h)$ in space.

$$\mathbf{q}^{(1)}(\mathbf{h}) = -D^{(1)}\mathbf{K}_D(\mathbf{h})D^{(1)}\mathbf{h} - D^{(1)}\mathbf{K}(\mathbf{h}) \tag{20}$$

Let $\Theta(\mathbf{h}) = (\theta \circ \mathbf{h}_1, \theta \circ \mathbf{h}_2, , \ldots, \theta \circ \mathbf{h}_M)^\top$ and $\mathbf{f} = (f(z_1, t), f(z_2, t), \ldots, f(z_M, t)$ be the values respectively of the moisture content $\theta(h)$ and the source function f at the

centers $z_i,\ i = 1, 2, \ldots, M$. The numerical resolution of Richards' equation (9)-(13) can then resume to the resolution of the following problem in time:

$$\frac{\mathrm{d}\Theta(\mathbf{h})}{\mathrm{d}t} = \mathcal{F}(\mathbf{h}), \quad t \in]0, T] \tag{21}$$

$$\mathbf{h}(0) = \mathbf{h}_0 \tag{22}$$

with

$$\mathcal{F}(\mathbf{h}) = \mathbf{q}^{(1)}(\mathbf{h}) + \mathbf{f} \tag{23}$$

and

$$\mathbf{h}_0 = (h_{init}(z_1), h_{init}(z_2), \ldots, h_{init}(z_M))^\top.$$

3.3. Time discretization. In this section, we want to approximate the problem in time (21)-(23). To do this we will use the implicit Euler method.

Let $t_n = n\delta t,\ n = 0, 1, \ldots, N$ a discretization of the time interval $[0, T]$, $\delta t = T/(N-1)$ the time-step size and $\Theta^n,\ \mathcal{F}^n$ the approximations of $\Theta(\mathbf{h}^n, t_n)$ and $\mathcal{F}(\mathbf{h}^n, t_n)$ with $\mathbf{h}^n = \mathbf{h}(t_n)$, $n = 0, 1, \ldots, N$.

The approximation of the equation (21) by a implicit Euler scheme gives

$$\frac{\Theta^{n+1} - \Theta^n}{\delta t} = \mathcal{F}^{n+1}, \quad n = 0, 1, \ldots, N-1. \tag{24}$$

The terms Θ^{n+1} and $\mathcal{F}^{n+1}$ cause equation (24) to be highly nonlinear. To overcome this nonlinearity problem, it will be necessary to use a linearization process. In our case we will use the Newton's iterative method.

3.4. Linearization. Let's denote $\Theta^{n+1,m+1}, \mathbf{K}_D^{n+1,m+1}$ and $\mathbf{K}^{n+1,m+1}$ the approximated values $\Theta(\mathbf{h}^{n+1,m+1}), \mathbf{K}_D(\mathbf{h}^{n+1,m+1})$ and $\mathbf{K}(\mathbf{h}^{n+1,m+1})$ in which $\mathbf{h}^{n+1,m+1}$ is the searched value of $\mathbf{h}^{n+1}$ in the stage $m+1$ of Newton's iterative process. Let's also denote $\mathbf{h}^{n+1,m}$ the value of $\mathbf{h}^{n+1}$ at the previous stage m,

$$\mathcal{F}(\mathbf{h}^{n+1,m}, \mathbf{h}^{n+1,m+1}) = -D^{(1)}\mathbf{K}_D^{n+1,m} D^{(1)}\mathbf{h}^{n+1,m+1} - D^{(1)}\mathbf{K}^{n+1,m} + \mathbf{f}^{n+1} \tag{25}$$

and

$$\mathcal{R}(\mathbf{h}^{n+1,m}, \mathbf{h}^{n+1,m+1}) = \frac{\Theta^{n+1,m+1} - \Theta^n}{\delta t} - \mathcal{F}(\mathbf{h}^{n+1,m}, \mathbf{h}^{n+1,m+1}) \tag{26}$$

If we use a one-order Taylor's series development of $\Theta^{n+1,m+1}$, we obtain the following approximation

$$\Theta^{n+1,m+1} \simeq \Theta^{n+1,m} + \frac{\mathrm{d}\Theta^{n+1,m}}{\mathrm{d}\mathbf{h}}\delta\mathbf{h}^{n+1} \tag{27}$$

where

$$\delta\mathbf{h}^{n+1} = \mathbf{h}^{n+1,m+1} - \mathbf{h}^{n+1,m} \tag{28}$$

$C(h) = \frac{\mathrm{d}\theta}{\mathrm{d}h}$ is the specific water capacity. Therefore, if we denote $\mathbf{C}^{n+1,m}$ the value of C in the approximated vector $\mathbf{h}^{n+1,m}$ then the approximation (27) can be rewritten as following:

$$\Theta^{n+1,m+1} \simeq \Theta^{n+1,m} + \mathbf{C}^{n+1,m}\delta\mathbf{h}^{n+1} \tag{29}$$

We then replace $\Theta^{n+1,m+1}$ in equation (27) by its expression given by (29) and therefore we obtain the new expression of $\mathcal{R}(\mathbf{h}^{n+1,m}, \mathbf{h}^{n+1,m+1})$ as following:

$$\mathcal{R}(\mathbf{h}^{n+1,m}, \mathbf{h}^{n+1,m+1}) = \frac{1}{\delta t}\mathbf{C}^{n+1,m}\delta\mathbf{h}^{n+1} + \frac{\Theta^{n+1,m} - \Theta^n}{\delta t} - \mathcal{F}(\mathbf{h}^{n+1,m}, \mathbf{h}^{n+1,m+1}) \tag{30}$$

The resolution of nonlinear problem (24) with the Newton's iterative method consists in solving at each time-step $n+1$ and at each stage $m+1$, the equation

$$J\ \delta\mathbf{h} = -\mathcal{R}(\mathbf{h}^{n+1,m}, \mathbf{h}^{n+1,m}) \tag{31}$$

where J is Jacobian matrix of $\mathcal{R}$ in $\mathbf{h}^{n+1,m}$ expressed as

$$J = \frac{\mathrm{d}\mathcal{R}}{\mathrm{d}\mathbf{h}}(\mathbf{h}^{n+1,m}, \mathbf{h}^{n+1,m}) = \frac{1}{\delta t}\mathbf{C}^{n+1,m} - D^{(1)}\mathbf{K}_D(\mathbf{h}^{n+1,m})D^{(1)} \tag{32}$$

until $\|\delta\mathbf{h}^{n+1}\|$ is below a certain tolerance *tol* or that m exceeds a maximum value *maxiter*.

Algorithm 1 describes how the Richards equation is solved at each time-step $n+1$ by Newton's iterative method.

Algorithm 1 NEWTON'S ITERATIVE METHOD TO COMPUTE h^{n+1}, THE VALUE OF h AT THE NEXT TIME STEP $n+1$.

Require: $\mathbf{h}^n, maxiter, tol$
  $\mathbf{h}^{n+1,0} = \mathbf{h}^n$
  while $m \leqslant maxiter$ **and** $\left\|\delta\mathbf{h}^{n+1}\right\| > tol$ **do**
    Solve the system (31) to obtain $\delta\mathbf{h}^{n+1}$
    $\mathbf{h}^{n+1,m+1} = \mathbf{h}^{n+1,m} + \delta\mathbf{h}^{n+1}$
    $m = m + 1$
  end while
  $\mathbf{h}^{n+1} = \mathbf{h}^{n+1,m+1}$
Ensure: $\mathbf{h}^{n+1}$

4. Numerical results

This section is to illustrate some numerical results of the Richards equation that we obtained using the numerical RBF-MQ method described in the previous section. These results are based on tests already performed by some authors such as Haverkamp, Polman, Van-Genushten Vogel and al. and can be found in ([4],[31],[30],[3],[7], [34])). The first test case concerns numerical results with analytical solutions. This will aim to show the numerical convergence of our method. The other following test cases show the conformity of the results we have obtained with those existing in the literature.

4.1. Tests with analytical solutions. Here we resume tests with analytical solutions that were performed by Sochala [30], to verify the numerical convergence of the RBF-MQ scheme that we developed for solving the Richards equation.

4.1.1. *Unsaturated test case.* We consider an unsaturated medium represented by a domain $\Omega = [0.20]$ and a simulation time interval $[0, 100]$. The analytical solution of this test is given by:

$$h(z,t) = 20.4\tanh(0.5(z + t/12 - 15)) - 41.5 \tag{33}$$

The hydrodynamic properties of soil $\theta(h)$ and $K(h)$ are given by:

$$\theta(h) = \frac{\theta_s - \theta_r}{1 + |\tilde{\alpha}h|^{\beta}} + \theta_r\ ; \qquad K(h) = \frac{K_s}{1 + |\tilde{A}h|^{\gamma}} \tag{34}$$

where
$\theta_s = 0.287, \quad \tilde{\alpha} = 0.0271\ cm^{-1}, \quad K_s = 9.44 \cdot 10^{-3}\ cm \cdot s^{-1}, \quad \gamma = 4.74,$
$\theta_r = 0.075, \quad \beta = 3.96, \quad \tilde{A} = 0.0524\ cm^{-1}$
and Dirichlet conditions are applied on the boundaries.

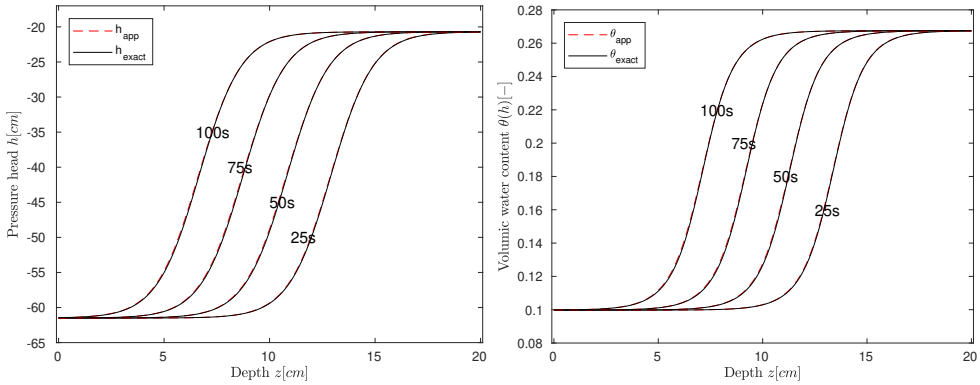

FIGURE 1. *Unsaturated test case*: On the left, the curve of pressure head h with respect to depth z and on the right the curve of the moisture content θ with respect to depth z. The number of discretization point in time is $N_t = 200$ and $N_z = 150$ in space. The shape parameter value is $c = 0.95$. The dashed line represent the approximate solution and those in continuous lines represent the exact solution.

The figure (2-1) shows that the relative error of the approximation of the pressure head h by the RBF-MQ method in space and Implicit Euler in time decreases as the time-step size becomes smaller. Similarly the figure (2-2) shows that approximation error decrease when the number of spatial discretization points are increased and is order 10^{-3}. When the number of time discretization is reduced to a certain level, the approximation of h become less accurate and the error become close to the order 10^{-2}. Figure(2-3) shows which values of the shape parameter c provide better accuracy. For small values of N_z, larger values of c are required to obtain good accuracy while for large N_z accuracy is already good for values of c in the neighbourhood 0.2 and more.

4.1.2. *Variably saturated test case.* The medium is assumed to be variably saturated on the same domain and during the same simulation period as in the previous test. The hydrodynamic properties of soil are the same as in previous test. Dirichlet boundary conditions are also applied to the edges of the domain and the analytical solution is given by:

$$h(z,t) = 20.4 \tanh(0.5(z + t/12 - 15)) + t/4 - 41.5. \tag{35}$$

It should be noted that in this test and in the previous test, the simulations were made with the source terms f in (9) necessary that the analytical solution h in (33) and (35) solve the problem (9). The calculation of f can be done simply with a computer program. In our case we used the software **SageMaths**.

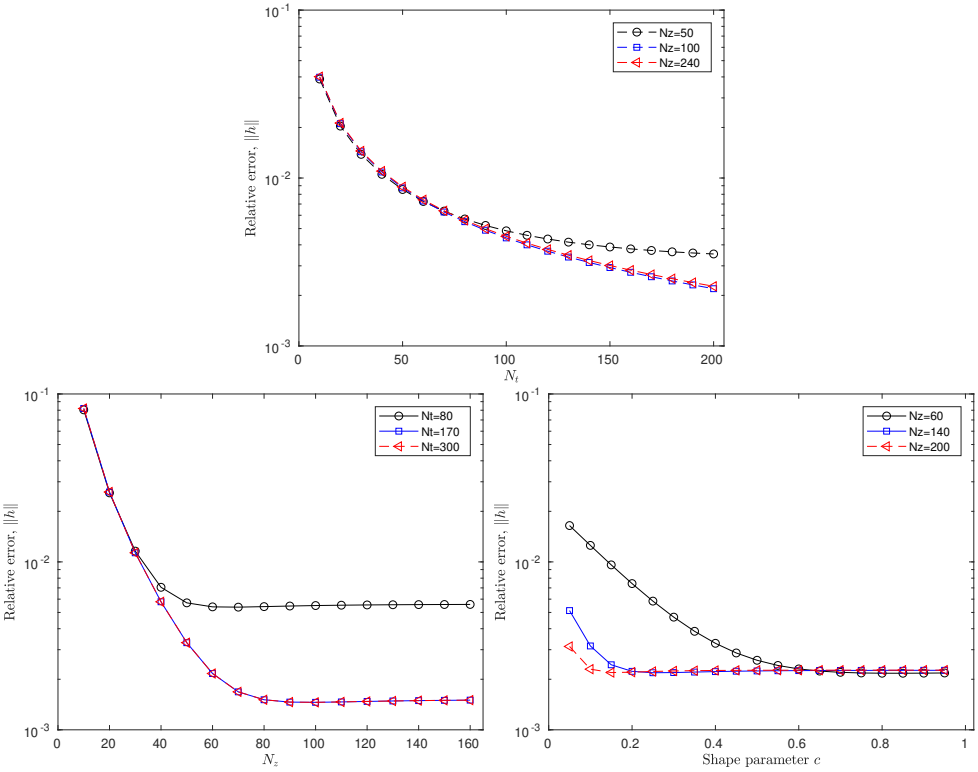

FIGURE 2. *Curves of errors in the unsaturated test case*: Representative curves of ℓ_2 relative norm errors of the approximation of h, with respect to the number of temporal discretization points N_t in figure (2-1), with respect to the number of discretization points in space N_z in figure (2-2) and with respect to the values of shape parameter c taken in the interval $]0, 1[$ with $N_t = 200$ in figure (2-3).

Figures (4) have almost the same characteristics as (2), except that to obtain a better accuracy, the number of points in space and in times must be relatively higher in the variably saturated case than in the saturated case.

4.2. Haverkamp test case. This test was performed by Haverkamp [4] and then performed in two space dimension by several authors including Celia and Bouloutas [3], Manzini and Ferraris [7] and Sochala [30]. This is a water flow in a vertical soil column of 40 cm deep. An initial condition $h(z, 0) = -61.5\ cm$ is applied to this column. Constant hydraulic pressure are applied at the column top ($h(40\ cm, t) = -20.7\ cm$) and below ($h(0, t) = -61.5\ cm$). The height of the column is positively oriented upwards. The hydrodynamic parameters are given by (34).

4.3. Polmann test case. This test was also considered by Celia and Bouloutas [3], Manzini and Ferraris [7] then Pierre Sochala [6]. The soil column is 10 m deep. Initially a pressure of 10 m is imposed on the whole length of the column, including

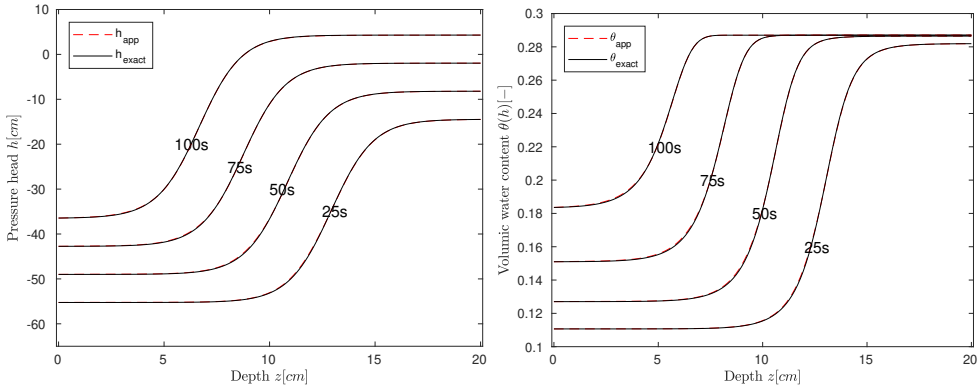

FIGURE 3. *Variably saturated test case*: On the left, the curve of pressure head h with respect to depth z and on the right the curve of the moisture content θ with respect to depth z. The number of discretization point in time is $N_t = 200$ and $N_z = 150$ in space. The shape parameter value is $c = 0.95$. The dashed line represent the approximate solution and those in continuous lines represent the exact solution.

			Unsaturated case	Variably saturated case
$c = 0.95$	N_t	N_z	relative error	relative error
	50	10	$6.06 \cdot 10^{-2}$	–
		70	$8.75 \cdot 10^{-3}$	$6.96 \cdot 10^{-3}$
		150	$8.84 \cdot 10^{-3}$	$6.98 \cdot 10^{-3}$
		250	–	–
	100	10	$6.17 \cdot 10^{-2}$	–
		70	$4.42 \cdot 10^{-3}$	$3.60 \cdot 10^{-3}$
		150	$4.49 \cdot 10^{-3}$	$3.60 \cdot 10^{-3}$
		250	–	–
	400	10	$6.26 \cdot 10^{-3}$	–
		70	$1.11 \cdot 10^{-3}$	$1.86 \cdot 10^{-3}$
		150	$1.13 \cdot 10^{-3}$	$1.82 \cdot 10^{-3}$
		250	–	–

TABLE 2. The relative error of the approximate hydraulic pressure head h for unsaturated case test and variably saturated case test: shape parameter $c = 0.95$.

the bottom while at the top, the imposed pressure is $-75\ cm$. Which is equivalent to an overpressure of $9.25\ m$.

The hydrodynamic properties of the soil are obtained from the following relations of Van Genuchten:

$$\theta(h) = \frac{\theta_s - \theta_r}{(1 + (\epsilon|h|)^n)^m} + \theta_r \ ; \qquad K(h) = K_s \frac{(1 - (\epsilon|h|)^{n-1}(1 + (\epsilon|h|)^n)^{-m})^2}{(1 + (\epsilon|h|)^n)^{\frac{m}{2}}} \tag{36}$$

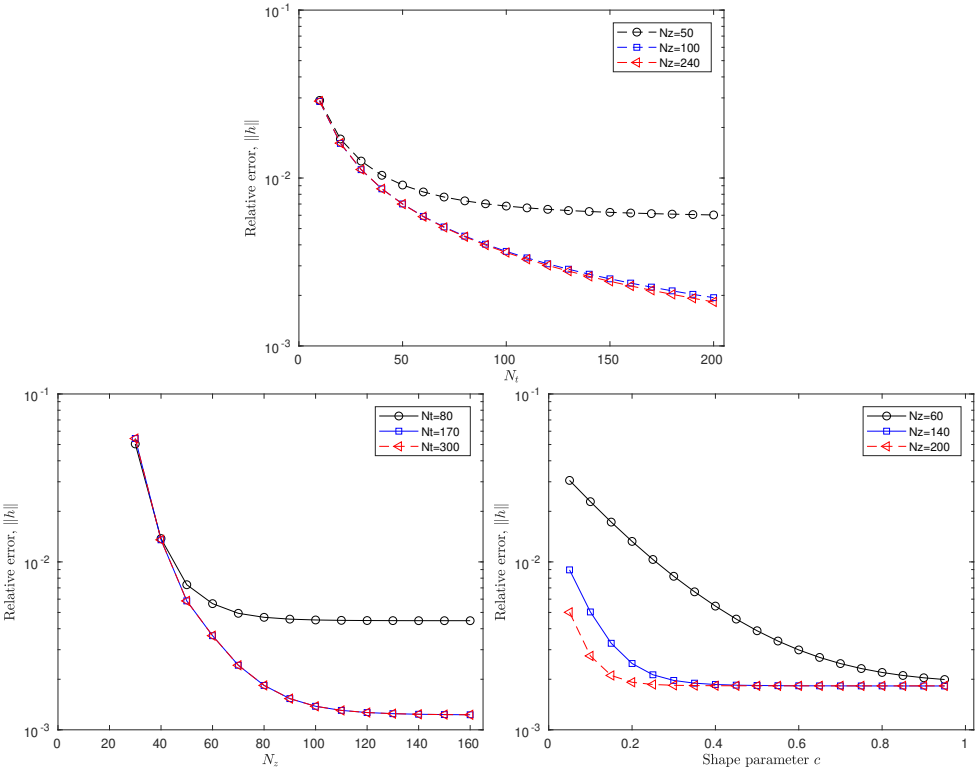

FIGURE 4. *Curves of errors in the variably saturated test case*: Representative curves of ℓ_2 relative norm errors of the approximation of h, with respect to the number of temporal discretization points N_t in figure (4-1), with respect to the number of discretization points in space N_z in figure (4-2) and with respect to the values of shape parameter c taken in the interval $]0, 1[$ with $N_t = 200$ in figure (4-3).

with $\theta_s = 0.368, \quad \epsilon = 0.0335\ cm^{-1}, \quad n = 2,$
$\theta_r = 0.102, \quad K_s = 9.22 \cdot 10^{-3}\ cm \cdot s^{-1}, \quad m = 0.5.$

The numerical results found in ([3],[30]) show parasitic oscillations because of the stiffness of the infiltration front. The use of a flux limiter by Sochala ([30]) allowed to reduce its oscillations without being able to eliminate them completely.

As can be seen, the RBF-MQ method in space and the Euler method implicit in time made it possible to suppress the parasitic oscillations caused by the stiffness of the infiltration font.

4.4. Vogel, Van-Genuchten and Cislerova cases test. These are three tests from articles by Vogel, Van Genuchten and Cilerova [31]. The hydrodynamic properties of the soil are given by modified Van Genuchten relations [32] in which a parameter h_s is considered here as the minimum capillary height. The tests are done on a vertical column height 1 m: $\Omega = [0, 100]$. For these tests, the simulation times T are respectively 1 day, a half-day and 2 days and the initial condition imposed for each

			Unsaturated case	Variably saturated case
$c = 0.5$	N_t	N_z	relative error	relative error
	50	10	$7.94 \cdot 10^{-2}$	–
		70	$8.56 \cdot 10^{-3}$	$7.29 \cdot 10^{-3}$
		250	$8.86 \cdot 10^{-3}$	$7.00 \cdot 10^{-3}$
		300	$8.87 \cdot 10^{-3}$	$7.00 \cdot 10^{-3}$
	200	10	$8.16 \cdot 10^{-2}$	–
		70	$2.27 \cdot 10^{-3}$	$2.79 \cdot 10^{-3}$
		150	$2.25 \cdot 10^{-3}$	$1.83 \cdot 10^{-3}$
		250	$2.27 \cdot 10^{-3}$	$1.83 \cdot 10^{-3}$
	400	10	$8.21 \cdot 10^{-3}$	–
		70	$1.44 \cdot 10^{-3}$	$2.28 \cdot 10^{-3}$
		250	$1.14 \cdot 10^{-3}$	$9.22 \cdot 10^{-4}$
		300	$1.14 \cdot 10^{-3}$	$9.22 \cdot 10^{-4}$

TABLE 3. The relative error of the approximate hydraulic pressure head h for unsaturated case test and variably saturated case test: shape parameter $c = 0.5$.

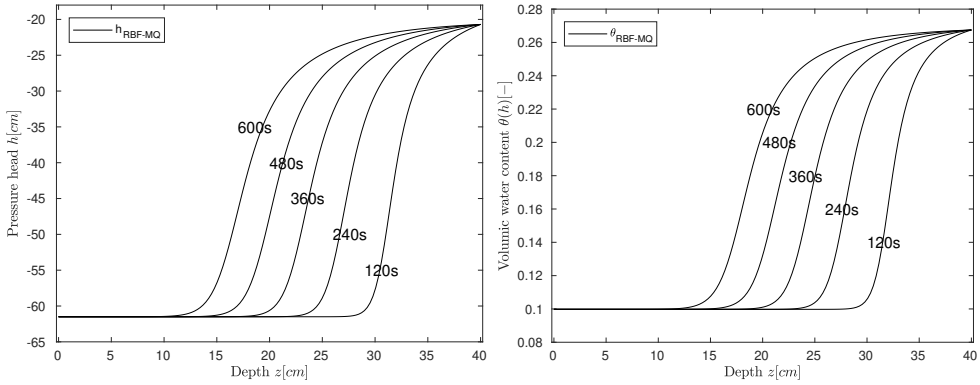

FIGURE 5. *Haverkamp test case*: Representative curves of the pressure head h on the left and those of the volumic water content $\theta(h)$ on the right. $N_t = 200$, $N_z = 140$, $c = 0.9$.

of these tests is:

$$h_0 = -10m - z \quad \text{in} \quad \Omega$$

$$\theta(h) = \tilde{\theta}(\theta_s - \theta_r) + \theta_r \; ; \qquad K(h) = K_s \tilde{\theta}^{\frac{1}{2}} \frac{(1 - (1 - (\tilde{\theta}/\beta)^{1/m})^m)^2}{(1 - (1 - (1/\beta)^{1/m})^m)^2} \tag{37}$$

with

$$\tilde{\theta} = \begin{cases} \dfrac{\beta}{(1 + (\epsilon|h|)^n)^m} & , \text{ if } \; h < -h_s \\ 1 & , \text{ otherwise.} \end{cases} \qquad \beta = (1 + (\epsilon h_s)^n)^m$$

$\theta_s = 0.38, \quad \epsilon = 0.008 \; cm^{-1}, \quad n = 1.09,$
$\theta_r = 0.068, \quad K_s = 5.55 \cdot 10^{-5} \; cm \cdot s^{-1}, \quad m = 0.0826.$

The boundary conditions are respectively:

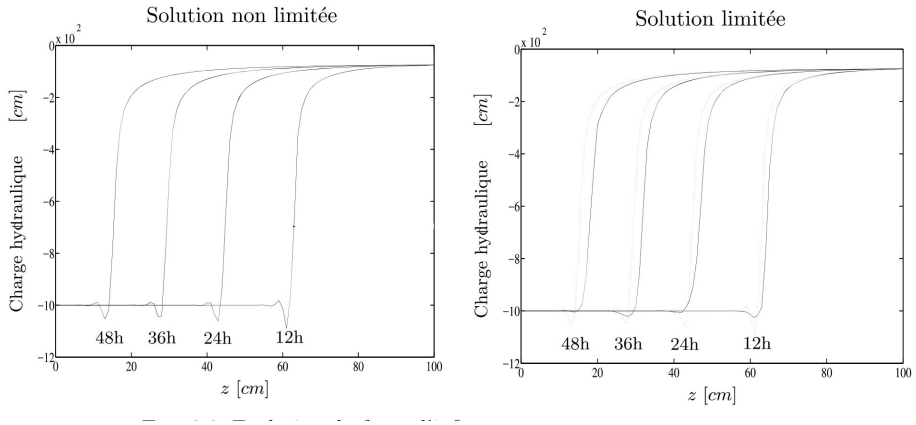

FIGURE 6. *Polmann test case (P. Sochala* [30]*).*

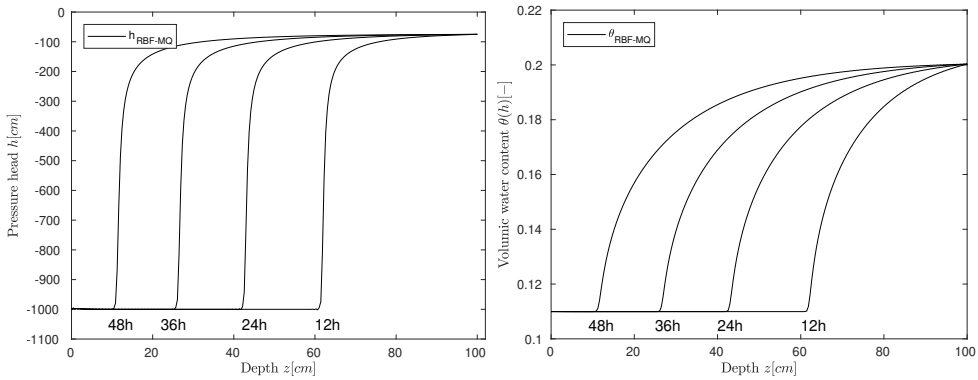

FIGURE 7. *Polmann test Case*: Representative curves of the pressure head h on the left and those of the volumic water content $\theta(h)$ on the right. $N_t = 200$, $N_z = 150$, $c = 0.95$.

CL1: $h_D = 0$ on $0 \times [0,T]$, $\quad q_N = 0$ on $100 \times [0,T]$
CL2: $q_N = 0$ on $0 \times [0,T]$, $\quad h_D = 0$ on $100 \times [0,T]$
CL3: $q_N = 0$ on $0 \times [0,T]$, $\quad q_N = 0$ on $100 \times [0,T]$

5. Conclusion

In this work, we have solved the mixed formulation of the Richards equation that models the flows in unsaturated porous media in dimension 1, using the RBF-MQ method. This is a method without mesh and relatively easier to program than mesh methods especially if the domain is complex. An implicit Euler scheme was used for temporal discretization. After comparing our case-by-case approach with exact solutions in unsaturated medium and in a variably saturated medium, we tested it on existing experimental examples in the literature: the Polmann test, the Haverkamp

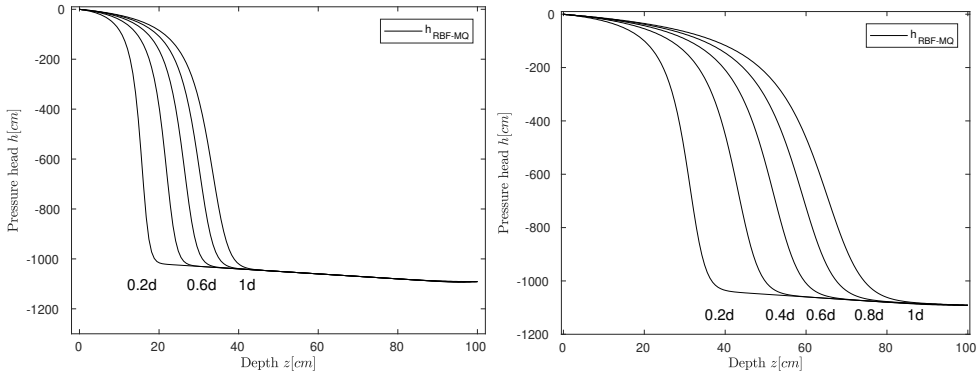

FIGURE 8. *Test case 1*: Simulation time $T = 1$ *day*, with **CL1** boundary conditions imposed on the edges. On the left, the curve of the pressure head h for $h_s = 10^{-3}cm$ and on the right for $h_s = 2cm$. $N_t = 300$, $N_z = 150$, $c = 0.95$.

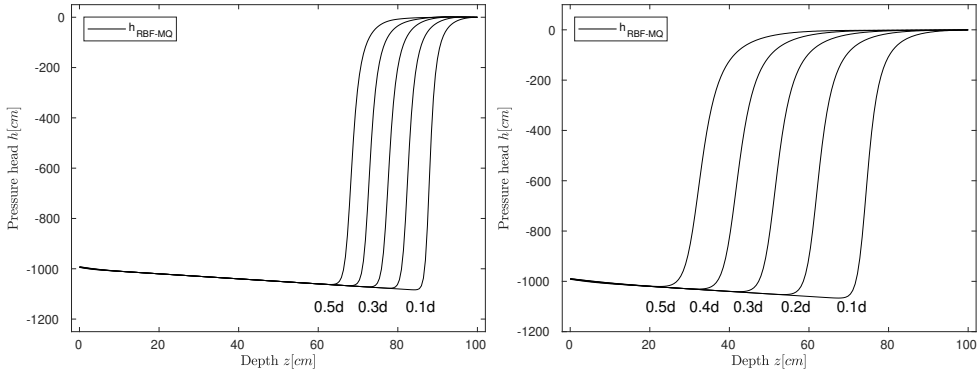

FIGURE 9. *Test case 2*: Simulation time $T = 1$ *day*, with **CL2** boundary conditions imposed on the edges. On the left, the curve of the pressure head h for $h_s = 10^{-3}cm$ and on the right for $h_s = 2cm$. $N_t = 200$, $N_z = 170$, $c = 0.95$.

test, the Vogel test , the Van-Genuchten test and the Cislerova test. For the Polmann test, the numerical methods used in the literature caused oscillations of the infiltration front. The method used in this work allowed correcting these oscillations. The other tests are in accordance with the tests found in the literature. All these results obtained prove the effectiveness of our approach.

References

[1] H. Darcy, *Les fontaines publiques de la ville de Dijon: exposition et application*, Victor Dalmont, 1856.

[2] L.A. Richards, Capillary conduction of liquids through porous mediums, *Physics* **1** (1931), 318–333.

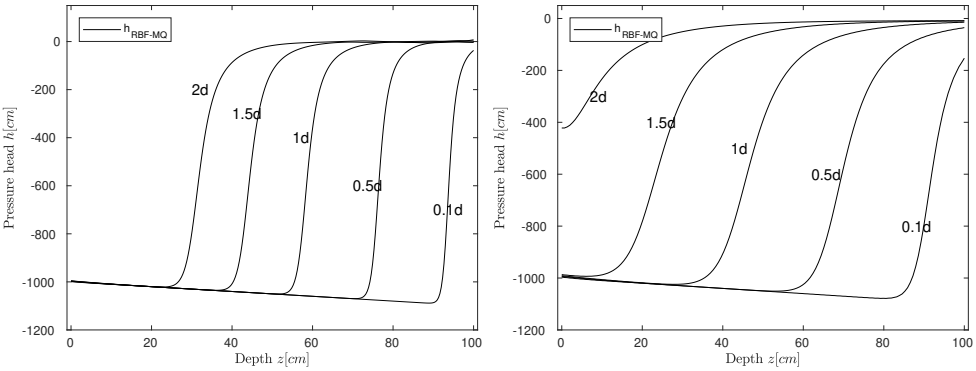

FIGURE 10. *Test case 3*: Simulation time $T = 0.5$ *day*, with **CL2** boundary conditions imposed on the edges. On the left, the curve of the pressure head h for $h_s = 10^{-3}cm$, $N_t = 200$, $N_z = 150$ and on the right for $h_s = 2cm$, $N_t = 400$, $N_z = 300$, $c = 0.95$.

[3] M.A. Celia, E.T. Bouloutas, R.L. Zarba, A general mass-conservative numerical solution for the unsaturated flow equation, *Water Resources Research* **26** (1990), 1483–1496.

[4] R. Haverkamp, M. Vauclin, J. Touma, P.J. Wierenga, G. Vachaud, A Comparison of Numerical Simulation Models For One-Dimensional Infiltration 1, *Soil Science Society of America Journal* **41** (1977), 285–294.

[5] M. Th. Van Genuchten, A closed-form equation for predicting the hydraulic conductivity of unsaturated soils 1, *Soil Science Society of America Journal* **44** (1980), 892–898.

[6] P. Sochala, A. Ern, S. Piperno, Mass conservative BDF-discontinuous Galerkin/explicit finite volume schemes for coupling subsurface and overland flows, *Computer Methods in Applied Mechanics and Engineering* **198** (2009), 2122–2136.

[7] G. Manzini, S. Ferraris, Mass-conservative finite volume methods on 2-D unstructured grids for the Richards' equation, *Advances in Water Resources* **27** (2004), 1199–1215.

[8] T.P. Clement, W.R. Wise, F.J. Molz, A physically based, two-dimensional, finite-difference algorithm for modeling variably saturated flow, *Journal of Hydrology* **161** (1994), 71–90.

[9] M. Bause, P. Knabner, Computation of variably saturated subsurface flow by adaptive mixed hybrid finite element methods, *Advances in Water Resources* **27** (2004), 565–581.

[10] M.W. Farthing, C.E. Kees, C.T. Miller, Mixed finite element methods and higher order temporal approximations for variably saturated groundwater flow, *Advances in Water Resources* **26** (2003), 373–394.

[11] M.D. Tocci, C.T. Kelley, C.T. Miller, C.E. Kees, Inexact Newton methods and the method of lines for solving Richards' equation in two space dimensions, *Computational Geosciences* **2** (1998), 291–309.

[12] W. Chen, Z.J Fu, C.S. Chen, *Recent advances in radial basis function collocation methods*, Springer, (2014).

[13] N.A. Libre, A. Emdadi, E.J. Kansa, M. Shekarchi, M. Rahimian, A fast adaptive wavelet scheme in RBF collocation for nearly singular potential PDEs, *Computer Modeling in Engineering and Sciences* **38** (2008), 263–284.

[14] R. Franke, Scattered data interpolation: tests of some methods, *Mathematics of Computation* **38** (1982), 181–200.

[15] E.J. Kansa, Multiquadrics – A scattered data approximation scheme with applications to computational fluid-dynamics – II solutions to parabolic, hyperbolic and elliptic partial differential equations, *Computers & Mathematics with Applications* **19** (1990), 147–161.

[16] E.J. Kansa, Multiquadrics – A scattered data approximation scheme with applications to computational fluid-dynamics – I surface approximations and partial derivative estimates, *Computers & Mathematics with applications* **19** (1990), 127–145.

[17] R.L. Hardy, Multiquadric equations of topography and other irregular surfaces, *Journal of geophysical research* **76** (1971), 1905–1915.
[18] J. Duchon, Splines minimizing rotation-invariant semi-norms in Sobolev spaces, In *Constructive theory of functions of several variables*, Springer (1977), 85–100.
[19] M.D. Buhmann, *Radial basis functions: theory and implementations*, Cambridge University Press, (2003).
[20] M. Buhmann, N. Dyn, Spectral convergence of multiquadric interpolation, *Proceedings of the Edinburgh Mathematical Society* **36** (1993), 319–333.
[21] S.A. Sarra, Adaptive radial basis function methods for time dependent partial differential equations, *Applied Numerical Mathematics***54** (2005), 79–94.
[22] J.M. Sanz-Serna, I. Christie, A simple adaptive technique for nonlinear wave problems, *Journal of Computational Physics* **67** (1986), 348–360.
[23] F. Motaman, G.R. Rakhshandehroo and M.R. Hashemi and M. Niazkar, Application of RBF-DQ Method to Time-Dependent Analysis of Unsaturated Seepage, *Transport in Porous Media* (2018).
[24] P.C.D. Milly, A mass-conservative procedure for time-stepping in models of unsaturated flow, *Advance in Water Ressources* **8** (1985), 32–36.
[25] K. Rathefelder, L. Abriola, Mass-conservative numerical solutions of the head-based Richards equation, *Water Resources Rechearch* **30** (1994), 2579–2586.
[26] D. Stevens, H. Power, A scalable and implicit meshless RBF method for the 3D unsteady nonlinear Richards equation with single and multi-zone domains, *Int. J. Numer. Methods Eng.* **85** (2011), 135–163.
[27] M. Dehghan, A. Shokri, Numerical solution of the nonlinear Klein?Gordon equation using radial basis functions, *J. Comput. Appli. Math.* **230** (2009), 400–410.
[28] P. Orsini, H. Power, M. Lees, H. Morvan, A control volume radial basis function techniques for the numerical, simulation of saturated flows in semi-confined aquifer, *Transp. Porous Media* **79** (2008), 171–196.
[29] B. Mavric, B. Sarler, Local radial basis function collocation method for linear thermoelasticity in two dimensions, *Int. J. Numer. Methods Heat Fluid Flow* **25** (2015), 1488–1510.
[30] P. Sochala, Méthodes numériques pour les écoulements souterrains et couplage avec le ruissellement, Ph.D. thesis, Paris Est (2008).
[31] T. Vogel, M. Th. Van Genuchten, M. Cislerova, Effect of the shape of the soil hydraulic functions near saturation on variably-saturated flow predictions, *Advances in Water Resources* **24** (2000), 133–144.
[32] M.G. Schaap, M. Th. Van Genuchten, A modified Mualem–van Genuchten formulation for improved description of the hydraulic conductivity near saturation, *Vadose Zone Journal* **5** (2006), 27–34.
[33] P. Sochala, A. Ern, Numerical methods for subsurface flows and coupling with runoff, *to appear*, 2013 M.G. Schaap and M. Th Van Genuchten, A modified Mualem–van Genuchten formulation for improved description of the hydraulic conductivity near saturation, *Vadose Zone Journal* **5** 2006, 27–34.
[34] V. Baron, Y. Coudière, P. Sochala, Comparison of DDFV and DG methods for flow in anisotropic heterogeneous porous media, *Oil & Gas Science and Technology–Revue d'IFP Energies nouvelles* **69** (2014), 673–686.
[35] P. Bastian, B. Riviere, Discontinuous Galerkin methods for two-phase flow in porous media, *University of Heidelberg Technical Report* **28** (2004).
[36] C. Grüninger, Discontinuous Galerkin methods for two-phase flows in porous media, Master thesis, Institute of Visualization and Interactive Systems, University of Stuttgart, (2010).

(P. O. F. Ouédraogo) University of Dédougou, BP 273, Dédougou, Burkina Faso
E-mail address: ouedraogo.opof.mail@gmail.com

([W. O. Sawadogo) University of Ouahigouya, Burkina Faso
E-mail address: wenddabo81@gmail.com

(O. So) Institute of Science, Burkina Faso
E-mail address: soousseni@gmail.com